

# GPR3 ligands discovered through combined virtual and conformational biosensor-based screening

Hannes Schihada\*<sup>[a]</sup>, Aida Shahraki<sup>[a]</sup> ‡, Ainoleena Turku<sup>[b]</sup> ‡,§, Maximilian Rath<sup>[c]</sup>, Lukas Wirth<sup>[c]</sup>, Hrisowalantu Tselepli<sup>[c]</sup>, Laura Heitzer<sup>[c]</sup>, Bernadette Vallaster<sup>[c]</sup>, Gunnar Schulte<sup>[b]</sup>, Daniel Hilger<sup>[a]</sup>, Steffen Pockes<sup>[c]</sup>, Martin J. Lohse\*<sup>[d]</sup>, and Peter Kolb\*<sup>[a]</sup>

[a] Philipps-Universität Marburg, Institute of Pharmaceutical Chemistry, Marbacher Weg 8, 35032 Marburg, Germany

[b] Section of Receptor Biology & Signaling, Department of Physiology and Pharmacology, Karolinska Institutet, 171 77 Stockholm, Sweden

[c] Institute of Pharmacy, University of Regensburg, Universitätsstraße 31, 93053 Regensburg, Germany

[d] ISAR Bioscience Institute, 82152 Planegg/Munich, Germany and TU München Klinikum Rechts der Isar, 81675 Munich

‡These authors contributed equally.

§Present address: Orion Pharma R&D, Orionintie 1A, 02101 Espoo, Finland

\* corresponding authors; hannes.schihada@uni-marburg.de; martin.lohse@isarbioscience.de; peter.kolb@uni-marburg.de

*GPR3, GPCR, conformational biosensor, virtual screening, medicinal chemistry.*

---

**ABSTRACT:** GPR3 belongs to the protein superfamily of G protein-coupled receptors (GPCRs) and plays a central role in both benign and malignant physiological processes, such as energy expenditure in adipocytes and Alzheimer's disease pathology, respectively. Despite the therapeutic potential of both receptor agonists and inverse agonists, GPR3 so far has lacked drug-like ligands and innovative screening technologies, hindering effective drug discovery efforts targeting this receptor. To overcome the limitations of conventional ligand screening techniques based on cAMP accumulation or  $\beta$ -arrestin recruitment, we developed a conformational GPR3 biosensor to monitor receptor activity in living cells with high-throughput screening (HTS)-compatible sensitivity and robustness. Combined with virtual compound screening against homology models of GPR3 and classical medicinal chemistry, this biosensor enabled us to identify new ligands, one of which (compound **33**) modulates GPR3-dependent  $G_s$  activity with nanomolar potency. Our study not only presents novel GPR3 ligands for future optimization efforts and paves the way for even further expansion of the GPR3 ligand repertoire, but our sensor approach also provides a blueprint for targeting other therapeutically attractive yet challenging orphan GPCRs.

---

## Introduction

Members of the protein superfamily of G protein-coupled receptors (GPCRs) are targeted by more than 30% of FDA-approved drugs. However, more than two-thirds of all non-olfactory GPCRs remain untapped for disease therapy, including many orphan GPCRs - receptors with yet unknown endogenous ligands. While one of the class A orphan GPCRs, GPR3, has only recently been deorphanized,<sup>1-3</sup> it still lacks drug-like ligands; moreover, innovative technologies to better study this receptor are just beginning to emerge<sup>4</sup>.

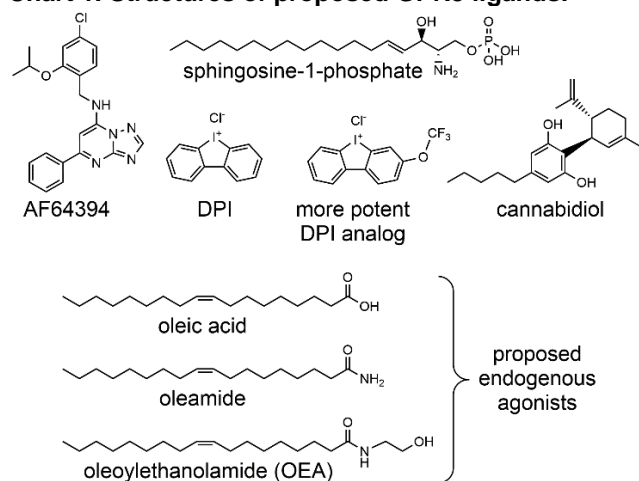
GPR3, together with GPR6 and GPR12, is part of a cluster of class A GPCRs that is phylogenetically related to receptors that bind sphingosine-1-phosphate (S1P), lysophosphatidic acid (LPA), cannabinoids and proopiomelanocortin-derived peptides. GPR3 activity is involved in both benign and malignant physiological processes. In the central nervous system (CNS), GPR3 mediates neurite outgrowth and neuronal cell survival<sup>5,6</sup> but has also been implicated in Alzheimer's disease<sup>7-10</sup>. In the

periphery, GPR3 regulates oocyte maturation and drives thermogenic programs in adipocytes<sup>11</sup>. These examples demonstrate that both agonists and inverse agonists of GPR3 may be of therapeutic value for various pathologies. Although researchers have been trying to discover molecules that target GPR3 for more than two decades, only a limited set of ligands that were validated in independent laboratories is currently available (**Chart 1**). While the activity of S1P and cannabidiol (CBD) on GPR3 remains questionable in light of conflicting reports<sup>12-16</sup>, AF64394 and its structural analogs have demonstrated their value as GPR3-specific inverse agonists<sup>4,17,18</sup>. In addition, diphenylethylideneiodonium chloride (DPI) is a proven synthetic agonist of GPR3 and a recently characterized DPI derivative promotes GPR3-dependent cAMP production with sub-micromolar potency<sup>12,19</sup>. In addition, the recent biochemical and structural studies revealed that endogenous long-chain lipids and fatty acids stabilize GPR3 in an active conformation<sup>1,2</sup>.

The very limited number of success stories illustrates that

today's GPR3-targeted drug discovery is still hampered by a poor understanding of the role of this receptor in cellular signaling and by a limited panel of assays that reveal GPR3 activity in living cells. This is emphasized by the fact that the few GPR3 ligands currently validated were discovered using one of only two available assay principles - cAMP accumulation or  $\beta$ -arrestin recruitment<sup>12,17,18</sup>. We thus reasoned that an innovative sensing approach is needed to facilitate tailored GPR3 ligand screening with higher success rates. Hence, we aimed to develop a sensor that detects compound-induced changes in GPR3 activity in a pathway-independent manner in a medium- to high-throughput screening (HTS) assay format. The latest generation of conformational GPCR sensors, based on bioluminescence resonance energy transfer (BRET) between NanoLuciferase (Nluc)<sup>20</sup> and HaloTag<sup>21</sup>, fulfills these criteria<sup>22-24</sup>. Here, we present the generation of the first conformational biosensor for an orphan GPCR with HTS-compatible sensitivity and robustness. We further demonstrate how this optical tool enabled us to identify new GPR3 ligands by combining virtual compound screening against 3D receptor models with a classical medicinal chemistry approach. Our most potent new GPR3 ligand is an inverse agonist that induces conformational changes in GPR3 with low micromolar potency and reduced basal  $G_s$  activity downstream of GPR3 with nanomolar potency.

**Chart 1. Structures of proposed GPR3 ligands.**



## Results and Discussion

### Design and validation of a conformational GPR3 sensor

To develop a conformational GPR3 biosensor that can be used in a microtiter well plate format, we employed the intramolecular BRET design previously validated for several class A GPCRs<sup>22-24</sup>. The BRET donor NanoLuc was fused to the receptor's full-length C-terminus and the self-labeling protein tag, HaloTag, was inserted into GPR3's third intracellular loop between amino acids Arg231 and His232 (**Fig. 1a**; protein sequence in **Fig. S1**). This GPR3-HaloTag/Nluc fusion construct even showed enhanced surface expression levels compared to wildtype GPR3, confirmed by whole-cell ELISA using the N-terminal HA-Tag of these GPR3 constructs (**Fig. 1b**). Upon expression of GPR3-HaloTag/Nluc in human embryonic kidney 293A cells (HEK293A), fluorescence labeling with the HaloTag@NanoBRET™ 618 ligand and addition of Nluc substrate furimazine, BRET in the receptor's basal conformation was indicated in the luminescence emission spectrum by the characteristic

acceptor peak around 620 nm (**Fig. 1c**). In addition, treatment with the GPR3 inverse agonist AF64394 resulted in a time- and ligand-concentration-dependent increase in BRET (**Fig. 1d, e**). The calculated  $EC_{50}$  value of 161 nM is similar to the affinity of AF64394 for N-terminally Nluc-fused GPR3<sup>4</sup> and to its previously determined potency of inhibiting GPR3 wildtype-mediated cAMP production<sup>17</sup>, demonstrating the functionality of this conformational GPR3 biosensor. Additionally, experiments with a GPR3-HaloTag/Nluc mutant with impaired AF64394 binding<sup>4</sup> (**Fig. 1e**) and with HaloTag/Nluc-based biosensors of the  $\alpha_{2A}$ - and  $\beta_2$ -adrenergic receptors ( $\beta_2AR$ )<sup>22</sup> further confirmed the specificity of the AF64394-induced response at this GPR3 biosensor (**Fig. S2**). To assess the suitability of this new sensor for medium- to high-throughput ligand screening, we measured its  $Z'$ -factor<sup>25</sup> in four independent experiments, confirming the high sensitivity (mean  $\pm$  SEM  $Z'$ -factor =  $0.78 \pm 0.02$ ) and low inter-day variability (coefficient of variation = 6.3%) (**Fig. 1f**). Ultimately, we also confirmed the signaling capacity of the GPR3 sensor using a cAMP biosensor<sup>26</sup> (**Fig. 1g**). These experiments revealed elevated basal levels of cAMP when GPR3-HaloTag/Nluc was co-expressed (**Fig. 1h**) and a concentration-dependent reduction of cAMP by AF64394 (**Fig. 1i**), demonstrating that the novel GPR3 conformational biosensor possesses GPR3 wildtype-like signaling capacity.

### Virtual screening for new GPR3 ligands

To demonstrate the value of this signaling pathway-independent readout of receptor activity for ligand discovery campaigns, we used the conformational biosensor to screen for GPR3 activity modulating compounds. To preselect the compounds to be tested *in vitro*, we conducted a structure-based *in silico* screening using molecular docking calculations<sup>27</sup>. At the time this study started, no experimental structures of GPR3 or the related receptors GPR6 and GPR12 were available. Hence, we constructed active- and inactive-state GPR3 homology models based on experimental structures of the phylogenetically related Cannabinoid receptor 1 (PDB IDs 6N4B and 5TGZ, respectively) (**Fig. S3a-c**). From exploratory docking calculations against the orthosteric pockets of both GPR3 models to assess their utility in a prospective screening, AF64394 and two structural analogs were ranked favorably compared to a randomly selected subset of our virtual compound library (about 700 molecules), indicating that the models were indeed able to recognize these GPR3 ligands (**Fig. S3d, e**). While encouraging, a recent experimental structure of GPR3 in complex with AF64394 shows that this ligand does not bind to the orthosteric pocket (Jun Xu, personal communication), hence we would not have included this step had the project been started today. A library of around 70,000 readily available compounds from the Chemical Biology Consortium Sweden (CBCS) was then docked to each of these structures (about 110,000 entries at pH  $7 \pm 2$ ). The docking poses of the top 100 (based on the docking score) molecules were visually inspected for each of the docking calculations to the active- and inactive-state GPR3 models. Additionally, the poses of 120 molecules from a consensus list (between the top 1000 molecules of either docking calculation) were evaluated. After this visual inspection followed a clustering of compounds based on 2D similarity to obtain a high structural diversity of compounds to be tested. Finally, 31 and 20 molecules were obtained from the lists resulting from docking to the inactive and active GPR3 model, respectively, and 42 compounds were obtained from the consensus list for *in vitro* testing.

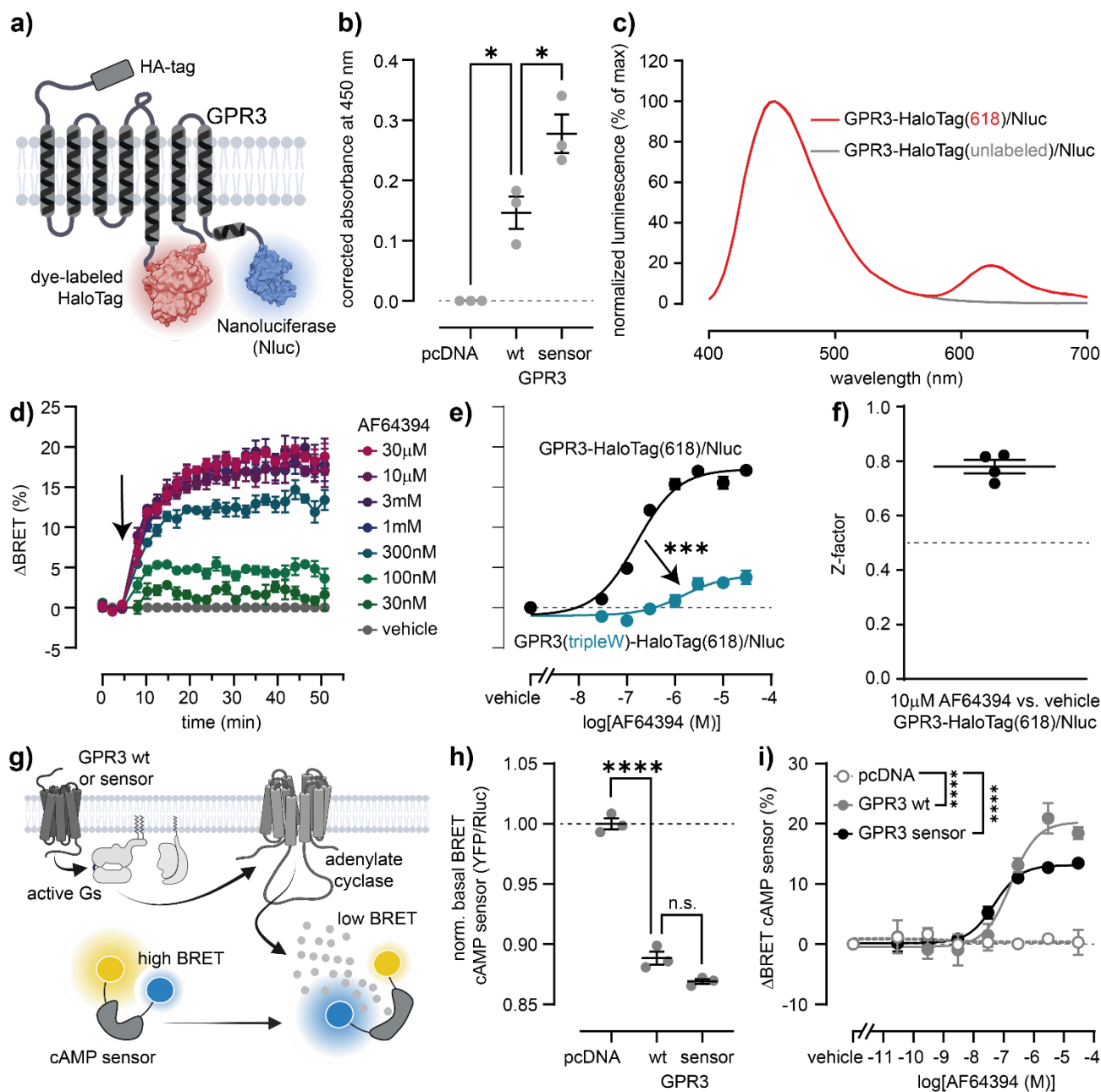


Figure 1. Development of a conformational GPR3 biosensor. a) Design of the conformational GPR3 biosensor. b) Surface expression of wildtype GPR3 and the GPR3 biosensor. c) Luminescence spectra of the HaloTag labeled and unlabeled GPR3 sensor. d) AF64394-induced  $\Delta$ BRET time course of the GPR3 biosensor. Arrow indicates the time point of AF64394 or vehicle addition. e) Concentration-response curves of AF64394 obtained with the GPR3 sensor and a mutant variant. f) Z-factor of the GPR3 biosensor. g) Scheme of the cAMP assay to assess the signaling capacity of the GPR3 biosensor. h) cAMP sensor BRET ratio upon co-expression of GPR3 sensor or wildtype. i) Concentration-response curves of AF64394 obtained with the cAMP biosensor in cells co-transfected with pcDNA, GPR3 wildtype or GPR3 sensor. All experiments were conducted in transiently (b - e, h, i) or stably (f) expressing HEK293A cells. Data show mean  $\pm$  SEM of three to four independent experiments. Statistical significance in (b) and (h) was tested using One-Way ANOVA followed by Tukey's multiple comparison. Statistical difference of  $\log$ EC<sub>50</sub> values in (e) and between the top plateaus in (i) was tested using the extra-sum-of-squares F-test. \*:  $p < 0.05$ , \*\*\*:  $p = 0.0002$ , \*\*\*\*:  $p < 0.0001$ .

#### *In vitro* testing of virtual hits

Initially, all 93 molecules were tested for activity at the GPR3 biosensor at a concentration of 1  $\mu$ M (Fig. 2a). Only three compounds induced a BRET response exceeding the threshold of the mean vehicle response  $\pm$  three-fold standard deviation and were subsequently applied at serial dilutions to cells expressing either GPR3- or  $\beta_2$ AR-HaloTag/Nluc<sup>22</sup> (Fig. S4a-c). All three

compounds induced GPR3-specific conformational changes. We hence searched for commercially available derivatives of these three molecules and obtained 14 additional compounds. Among these analogs, two more compounds induced GPR3-specific conformational changes (Fig. S4d-e). Of the five compounds that emerged from the virtual screen, three – hereafter referred to as virtual hit 1-3, VH1/2/3 – were selected for in-

house chemical synthesis (compounds **52**, **93**, and **115**; cf. **Scheme 1**, **Figure S5**), providing compounds of  $\geq 99\%$  purity for hit validation (NMR spectra: **Fig. S6-S141**; HPLC purity: **Fig. S142 - S217**). For VH1, the racemic mix, rac-VH1/**52**, was synthesized and used for testing. Compounds **52**, VH2/**93**, and

VH3/**115** (**Fig. S5**) were then validated with the GPR3 biosensor including  $\beta_2$ AR-HaloTag/Nluc as a negative control. All three compounds induced concentration-dependent and GPR3-specific conformational changes with potencies ranging from 25 (rac-VH1) to 85  $\mu$ M (VH3) (**Fig. 2b-d**).

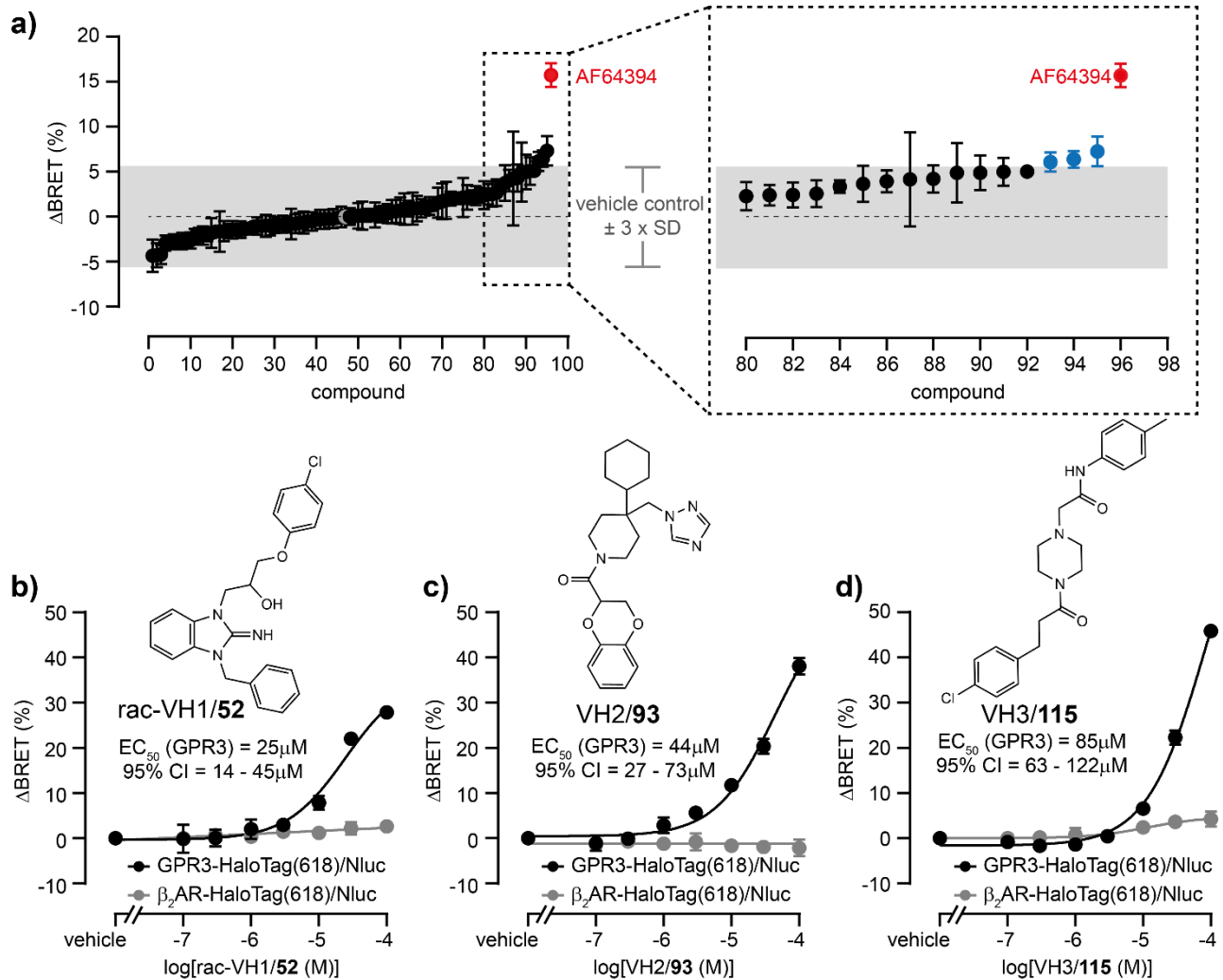
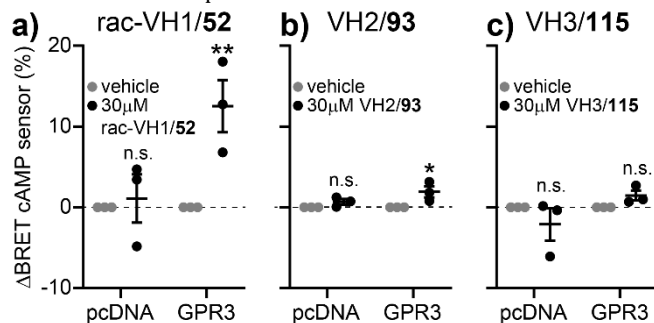


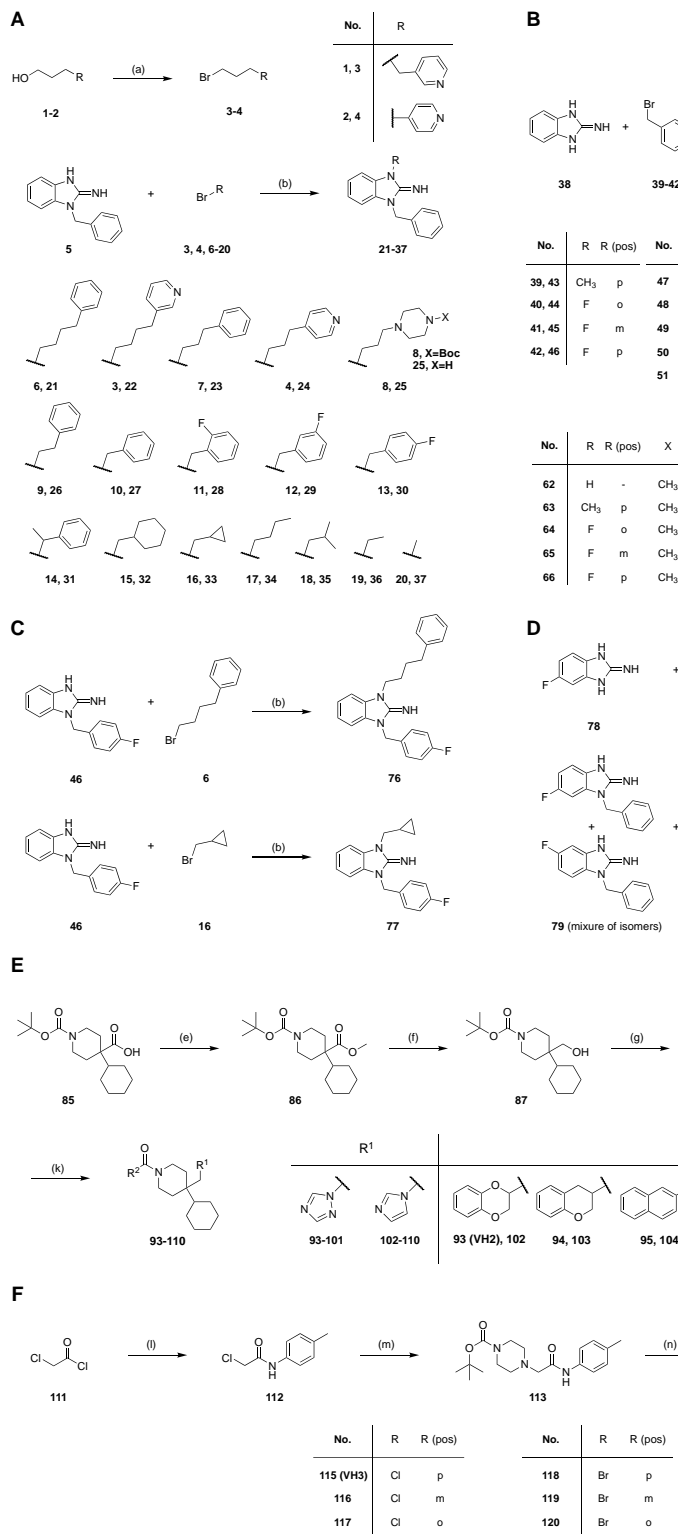
Figure 2. *In vitro* testing of virtual screening hits. a) BRET changes of GPR3-HaloTag(618)/Nluc induced by 93 ordered test compounds (1  $\mu$ M), vehicle control (grey) or 10  $\mu$ M AF64394 used as positive control. The grey shaded area indicates negative control  $\pm$  threefold SD. b-d) Concentration response curves of in-house synthesized rac-VH1/**52**, VH2/**93** and VH3/**115** obtained with the GPR3-HaloTag(618)/Nluc or  $\beta_2$ AR-HaloTag(618)/Nluc sensor used as a negative control. Data show mean  $\pm$  SEM of two (a) or three (b-d) independent experiments conducted in HEK293A cells stably expressing the indicated biosensors.

With the first GPR3 ligands identified by using a conformational readout in our hands, we next wanted to understand whether these compounds could have been detected in a cAMP-



based assay, which has been used extensively in the past to screen for GPR3 ligands. We therefore tested rac-VH1/**52**, VH2/**93** and VH3/**115** in cells expressing a cAMP biosensor. Interestingly, only rac-VH1 and - to a much lesser extent - VH2 induced GPR3-dependent changes in cAMP concentrations, demonstrating that a cAMP-based screen would likely have Figure 3. Effect of rac-VH1/**52**, VH2/**93** and VH3/**115** on GPR3-dependent cAMP production. a-c) BRET changes induced by vehicle control or 30  $\mu$ M rac-VH1/**52** (a), VH2/**93** (b) or VH3/**115** (c) in HEK293A cells transiently transfected with a cAMP BRET sensor along with pcDNA or GPR3. Data show mean  $\pm$  SEM of three independent experiments. Statistical significance was tested using Two-Way ANOVA followed by Sidak multiple comparison (\*:  $p < 0.05$ ; \*\*:  $p < 0.01$ ).

incorrectly classified VH3 as a nonbinder (**Fig. 3**).



Scheme 1. Synthesis of VH1-3 analogs 21-37 (A), 52-77 (B, C), 80-84 (D), 93-110 (E), and 115-124 (F). Reagents and conditions: (a) *N*-bromosuccinimide (1.2 eq), PPh<sub>3</sub> (1.2 eq), DCM, 4 h, 0 °C; (b) butan-2-one, 48 h, 90 °C; (c) 20 M NaOH, acetone, 2 h, 60 °C; (d) EtOH, 48 h, 100 °C; (e) CH<sub>3</sub>I (1.2 eq), K<sub>2</sub>CO<sub>3</sub> (3.0 eq), DMF, overnight, rt; (f) LiAlH<sub>4</sub> (2.0 eq), TFA, 4 d, 0 °C to rt; (g) methanesulfonyl chloride (2.0 eq), TEA (2.0 eq), DCM, overnight, 0 °C to rt; (h) sodium salt (3 eq), DMF, overnight, 110 °C; (i) 20 % TFA in DCM, overnight, 0 °C to rt; (k) bicyclic carboxylic acid (2.0 eq), DIPEA (3 eq), HATU (1.1 eq), DMF, overnight, rt; (l) 4-methylaniline (1 eq), TEA (2 eq), DCM, 4-6 h, 0 °C to rt; (m) *tert*-butyl-piperazine-1-carboxylate (3 eq), K<sub>2</sub>CO<sub>3</sub> (5.0 eq), CH<sub>3</sub>CN, 5 h, 80 °C; (n) 50 % TFA in DCM, 3 h, rt; (o) 3-phenylpropanoic acid derivative (1 eq), DIPEA (2-3 eq), HATU (1.2-1.5 eq), TEA (2 eq), DCM, 12 h, -15 °C.

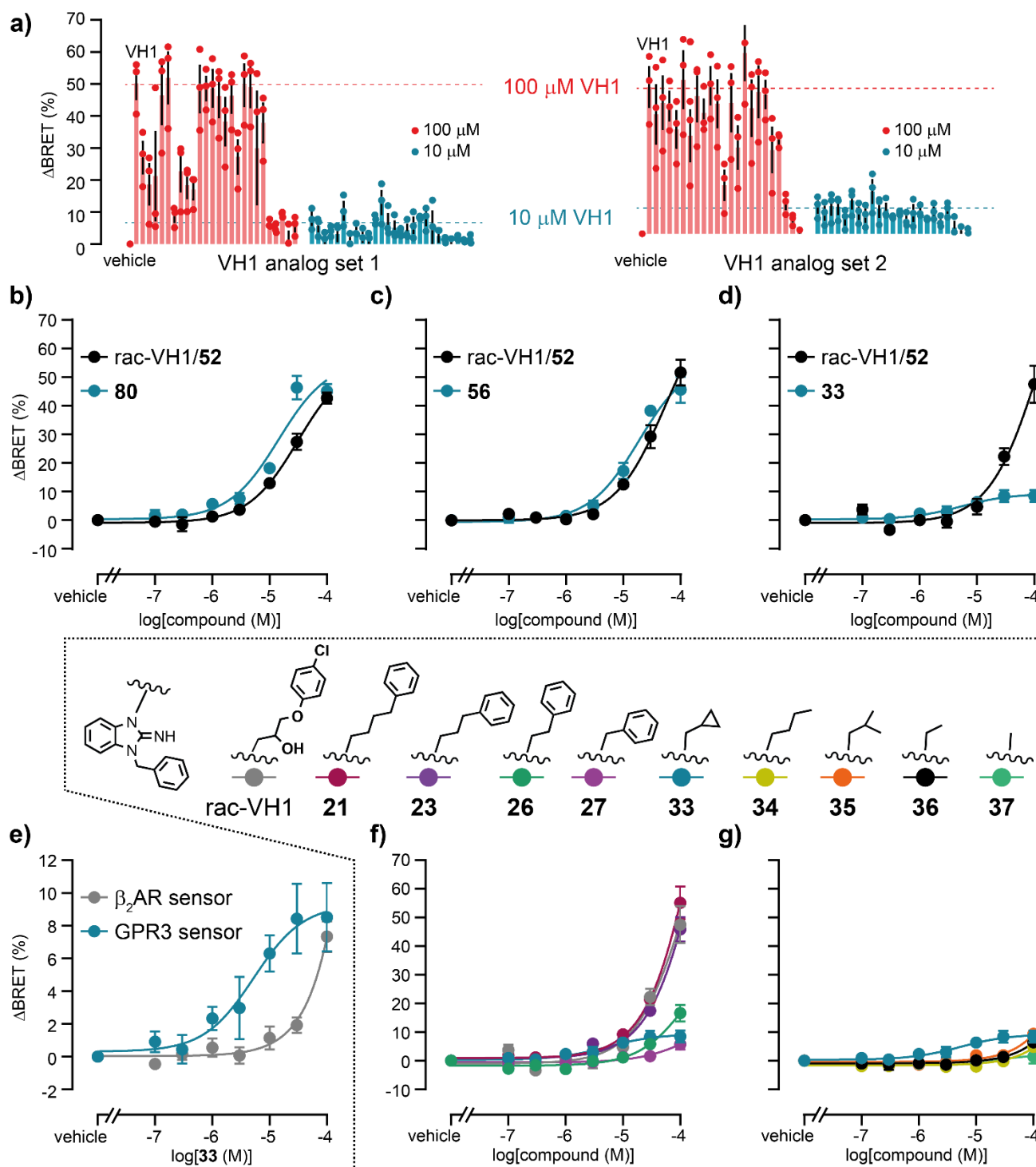


Figure 4. *In vitro* testing of VH1 analogs. a) BRET changes of GPR3-HaloTag(618)/Nluc induced by vehicle control, rac-VH1/52 and 49 chemical analogs. b-d) Concentration response curves of VH1 analogs **80** (b), **56** (c) and **33** (d) obtained with the GPR3-HaloTag(618)/Nluc sensor. e) Comparison of the **33** response at GPR3- vs.  $\beta_2$ AR-HaloTag(618)/Nluc sensor. f, g) Concentration response curves of rac-VH1/52 and its analogs **21**, **23**, **26**, **27**, **33**, and **34** – **37** obtained with the GPR3-HaloTag(618)/Nluc sensor. Data show mean  $\pm$  SEM of three independent experiments conducted in HEK293A cells stably expressing the indicated biosensor.



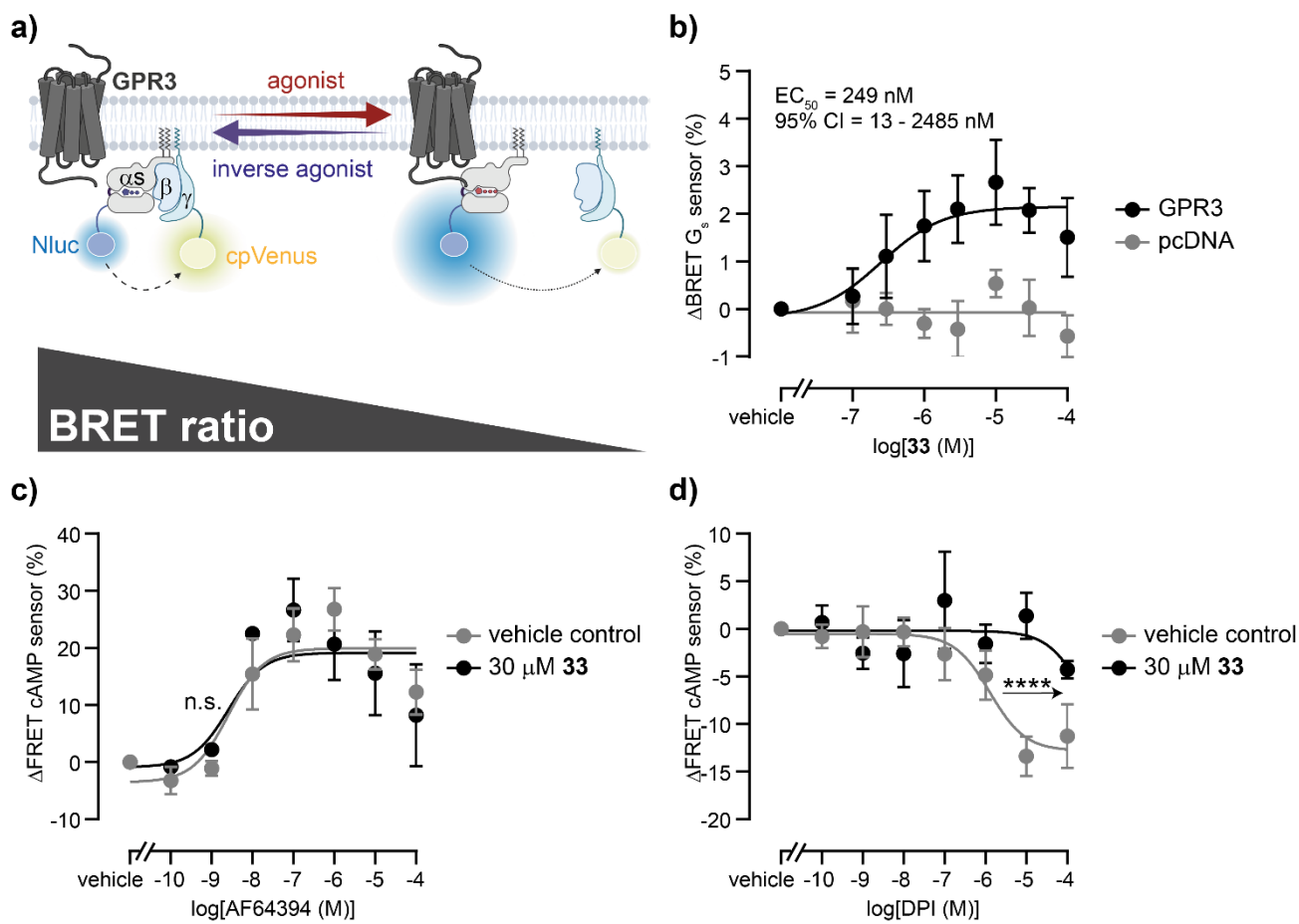


Figure 6. Compound **33** inhibits constitutive and ligand-dependent GPR3 signaling. a) Schematic of a live-cell  $G_s$  heterotrimer dissociation / re-association assay to assess GPR3-dependent  $G_s$  activity. b) Concentration response curves of **33** obtained with the  $G_s$  dissociation sensor in cells co-transfected with GPR3 or empty vector control (pcDNA). c-d) Concentration response curves of AF64394 (c) and DPI (d) obtained with a cAMP biosensor in cells co-expressing GPR3 and pretreated with 30  $\mu\text{M}$  **33** or vehicle control. Data show mean  $\pm$  SEM of three (c, d) or four (b) independent experiments conducted in HEK293A cells transiently expressing the indicated proteins. Extra-sum-of-squares F-test was performed to check for statistical difference of the  $EC_{50}$  values in (c) and (d) (\*\*\*\*:  $p < 0.0001$ ).

induced cAMP generation (Fig. 6d). These data support our previous observation that DPI and AF64394 engage distinct sites in GPR3<sup>4</sup> and suggest that **33** competes with DPI for GPR3 binding.

#### Physicochemical properties of **33**

Finally, we assessed the physicochemical properties of **33** using the SwissADME Swiss Drug Design online tool<sup>32</sup>. This analysis indicated that **33**, with a molecular weight of only 277 g/mol, a calculated Log-P of 2.9, no Lipinski rule violations, zero PAINS alerts, high leadlikeness and high synthetic accessibility (2.4 on a scale ranging from 1-10 / highly accessible-not accessible), provides ample room for synthetic expansions and modifications in future campaigns aiming for more potent and efficacious **33** analogs.

#### Conclusions

GPR3 is a class A GPCR that holds great potential for the development of treatments against severe human diseases. However, the therapeutic exploitation of this target is hampered by a very limited number of available GPR3 ligands. To fill this gap, we have developed an analytical tool that enables the discovery and characterization of new GPR3 ligands. Our biosensor detects ligand-induced conformational changes in GPR3 and

allowed us to identify and optimize new ligands by combining this advanced analytical tool with virtual compound screening and classical medicinal chemistry. Our virtual screening approach based on compound docking to 3D models of GPR3 revealed three chemically novel inverse agonists of GPR3, VH1-3. Subsequent synthesis of more than 70 VH1/2/3 analogs allowed us to further improve the potency of VH1 and identify one of its chemical analogs, **33**, as a GPR3 ligand with low micromolar potency in the conformational readout ( $EC_{50} = 5 \mu\text{M}$ ) and sub-micromolar potency in a signaling-based G protein re-association assay ( $EC_{50} = 249 \text{ nM}$ ). Additionally, mutagenesis studies and competition experiments with two known GPR3 ligands provided insights into the binding mode of **33** at GPR3. In the future, **33** may, due to its favorable chemical characteristics, serve as a useful lead structure for the development of advanced GPR3 inverse agonists that could aid in the treatment of severe, GPR3-dependent diseases such as Alzheimer's disease. Its low molecular weight, balanced physicochemical properties and high synthetic accessibility allows for extensive chemical derivatization towards further advanced GPR3 inverse agonists.

Collectively, our results demonstrate the power of structure-based ligand discovery pipelines including readily applicable

conformational GPCR biosensors. Using such tools, the modulation of receptor activity can be detected in a downstream signaling pathway-independent – and therefore unbiased – manner, reducing the risk of false screening results. This advantage is particularly relevant for poorly-studied targets, e.g., orphan GPCRs with often unknown signaling patterns, as exemplified by the discovery of VH3/115. VH3/115 modulates the conformation of GPR3 but not GPR3-dependent cAMP production. This provides evidence for an unproductive GPR3 conformation that is stabilized by VH3 or GPR3 signaling via  $G_{s-}$  and cAMP-independent pathways, possibilities that require further investigation.

## ASSOCIATED CONTENT

**Supporting Information.** The Supporting Information file includes the Materials and Methods section, amino acid sequence of the GPR3 biosensor, supporting experimental data, GPR3 homology model snapshots and validation data, and chemical synthesis information supplemented with the analytical data of new compounds. This material is available free of charge via the Internet at <http://pubs.acs.org>.

## AUTHOR INFORMATION

### Corresponding Authors

\* Peter Kolb; [peter.kolb@uni-marburg.de](mailto:peter.kolb@uni-marburg.de)  
\* Martin J. Lohse; [Martin.Lohse@isarbioscience.de](mailto:Martin.Lohse@isarbioscience.de)  
\* Hannes Schihada; [hannes.schihada@uni-marburg.de](mailto:hannes.schihada@uni-marburg.de)

### Author Contributions

The manuscript was written through contributions of all authors. All authors have given approval to the final version of the manuscript. H.S., G.S., S.P., M.J.L. and P.K.: resources; H.S., M.J.L. and P.K.: conceptualization; H.S., M.R., H.T., L.H., L.R., A.S., and A.T.: formal analysis; H.S., A.S., A.T., B.V., L.H.: investigation; H.S.: writing—original draft; L.H., B.V., H.T., M.R., L.W., S.P., A.S., and H.S.: visualization; H.S., S.P., M.J.L., and P.K.: funding acquisition; all authors: writing—review and editing; P.K., M.J.L., H.S., and S.P.: supervision; H.S., M.J.L., and P.K.: project administration.

### Funding Sources

This project has received funding from the European Union's Horizon 2020 research and innovation programme under the Marie Skłodowska-Curie grant agreement No 101062195. P.K. thanks the German Research Foundation DFG for Heisenberg professorships KO4095/4-1 and KO4095/5-1. S.P. thanks the German Research Foundation DFG for Heisenberg professorship PO 2563/4-1 and research grant PO 2563/5-1. The work at Karolinska Institutet was supported by the German Research Foundation DFG (427840891) and the Swedish Research Council (2019–01190).

## ACKNOWLEDGMENT

The authors thank Anna Krook at the Department of Physiology and Pharmacology, Karolinska Institutet, Stockholm, Sweden, for providing access to the ClarioStar plate reader; Ulrike Zabel at the Institute of Pharmacology and Toxicology, University of Wuerzburg, Germany, for cloning support and Sigurd Elz for providing the infrastructure at the University of Regensburg.

## ABBREVIATIONS

$\beta_2$ AR,  $\beta_2$ -adrenergic receptors; BRET, bioluminescence resonance energy transfer; CBD, cannabidiol; CNS, central nervous system; DPI, diphenylethylidone chloride; FRET, fluorescence resonance energy transfer; GPCR, G protein-coupled receptor; HEK293, human embryonic kidney; LPA, lysophosphatidic acid; Nluc, Nanoluciferase; S1P, sphingosine-1-phosphate (S1P).

## REFERENCES

- (1) Chen, G.; Staffen, N.; Wu, Z.; Xu, X.; Pan, J.; Inoue, A.; Shi, T.; Gmeiner, P.; Du, Y.; Xu, J. Structural and Functional Characterization of the Endogenous Agonist for Orphan Receptor GPR3. *Cell Research* **2024** *34:3* **2024**, *34* (3), 262–265. <https://doi.org/10.1038/s41422-023-00919-8>.
- (2) Xiong, Y.; Xu, Z.; Li, X.; Wang, Y.; Zhao, J.; Wang, N.; Duan, Y.; Xia, R.; Han, Z.; Qian, Y.; Liang, J.; Zhang, A.; Guo, C.; Inoue, A.; Xia, Y.; Chen, Z.; He, Y. Identification of Oleic Acid as an Endogenous Ligand of GPR3. *Cell Research* **2024** *34:3* **2024**, *34* (3), 232–244. <https://doi.org/10.1038/s41422-024-00932-5>.
- (3) Russell, I. C.; Zhang, X.; Bumbak, F.; McNeill, S. M.; Josephs, T. M.; Leeming, M. G.; Christopoulos, G.; Venugopal, H.; Flocco, M. M.; Sexton, P. M.; Wootten, D.; Belousoff, M. J. Lipid-Dependent Activation of the Orphan G Protein-Coupled Receptor, GPR3. *Biochemistry* **2024**, *63* (5), 625–631. <https://doi.org/10.1021/ACS.BIOCHEM.3C00647>.
- (4) Bresinsky, M.; Shahraki, A.; Kolb, P.; Pockes, S.; Schihada, H. Development of Fluorescent AF64394 Analogues Enables Real-Time Binding Studies for the Orphan Class A GPCR GPR3. *J Med Chem* **2023**. <https://doi.org/10.1021/acs.jmedchem.3c01707>.

- (5) Tanaka, S.; Ishii, K.; Kasai, K.; Yoon, S. O.; Saeki, Y. Neural Expression of G Protein-Coupled Receptors GPR3, GPR6, and GPR12 Up-Regulates Cyclic AMP Levels and Promotes Neurite Outgrowth\*. *Journal of Biological Chemistry* **2007**, *282* (14), 10506–10515. <https://doi.org/https://doi.org/10.1074/jbc.M700911200>.
- (6) Tanaka, S.; Miyagi, T.; Dohi, E.; Seki, T.; Hide, I.; Sotomaru, Y.; Saeki, Y.; Antonio Chiocca, E.; Matsumoto, M.; Sakai, N. Developmental Expression of GPR3 in Rodent Cerebellar Granule Neurons Is Associated with Cell Survival and Protects Neurons from Various Apoptotic Stimuli. *Neurobiol Dis* **2014**, *68*, 215–227. <https://doi.org/https://doi.org/10.1016/j.nbd.2014.04.007>.
- (7) Thathiah, A.; Horré, K.; Snellinx, A.; Vandeweyer, E.; Huang, Y.; Ciesielska, M.; De Kloe, G.; Munck, S.; De Strooper, B.  $\beta$ -Arrestin 2 Regulates A $\beta$  Generation and  $\gamma$ -Secretase Activity in Alzheimer's Disease. *Nat Med* **2013**, *19* (1), 44–49. <https://doi.org/10.1038/nm.3023>.
- (8) Huang, Y.; Guimarães, T. R.; Todd, N.; Ferguson, C.; Weiss, K. M.; Stauffer, F. R.; McDermott, B.; Hurtle, B. T.; Saito, T.; Saido, T. C.; MacDonald, M. L.; Homanics, G. E.; Thathiah, A. G Protein-Biased GPR3 Signaling Ameliorates Amyloid Pathology in a Preclinical Alzheimer's Disease Mouse Model. *Proc Natl Acad Sci U S A* **2022**, *119* (40). <https://doi.org/10.1073/PNAS.2204828119>.
- (9) Thathiah, A.; Spittaels, K.; Hoffmann, M.; Staes, M.; Cohen, A.; Horré, K.; Vanbrabant, M.; Coun, F.; Baekelandt, V.; Delacourte, A.; Fischer, D. F.; Pollet, D.; De Strooper, B.; Merchiers, P. The Orphan G Protein-Coupled Receptor 3 Modulates Amyloid-Beta Peptide Generation in Neurons. *Science (1979)* **2009**, *323* (5916), 946–951. <https://doi.org/10.1126/science.1160649>.
- (10) Huang, Y.; Skwarek-Maruszewska, A.; Horré, K.; Vandeweyer, E.; Wolfs, L.; Snellinx, A.; Saito, T.; Radaelli, E.; Corthout, N.; Colombelli, J.; Lo, A. C.; Van Aerschot, L.; Callaerts-Vegh, Z.; Trabzuni, D.; Bossers, K.; Verhaagen, J.; Ryten, M.; Munck, S.; D'Hooge, R.; Swaab, D. F.; Hardy, J.; Saido, T. C.; De Strooper, B.; Thathiah, A. Loss of GPR3 Reduces the Amyloid Plaque Burden and Improves Memory in Alzheimer's Disease Mouse Models. *Sci Transl Med* **2015**, *7* (309), 309ra164–309ra164. <https://doi.org/10.1126/scitranslmed.aab3492>.
- (11) Sveidahl Johansen, O.; Ma, T.; Hansen, J. B.; Markussen, L. K.; Schreiber, R.; Reverte-Salisa, L.; Dong, H.; Christensen, D. P.; Sun, W.; Gnad, T.; Karavaeva, I.; Nielsen, T. S.; Kooijman, S.; Cero, C.; Dmytriyeva, O.; Shen, Y.; Razzoli, M.; O'Brien, S. L.; Kuipers, E. N.; Nielsen, C. H.; Orchard, W.; Willemsen, N.; Jespersen, N. Z.; Lundh, M.; Sustarsic, E. G.; Hallgren, C. M.; Frost, M.; McGonigle, S.; Isidor, M. S.; Broholm, C.; Pedersen, O.; Hansen, J. B.; Grarup, N.; Hansen, T.; Kjær, A.; Granne-man, J. G.; Babu, M. M.; Calebiro, D.; Nielsen, S.; Rydén, M.; Soccio, R.; Rensen, P. C. N.; Treebak, J. T.; Schwartz, T. W.; Emanuelli, B.; Bartolomucci, A.; Pfeifer, A.; Zechner, R.; Scheele, C.; Mandrup, S.; Gerhart-Hines, Z. Lipolysis Drives Expression of the Constitutively Active

- Receptor GPR3 to Induce Adipose Thermogenesis. *Cell* **2021**, *184* (13), 3502–3518.e33.  
<https://doi.org/10.1016/j.cell.2021.04.037>.
- (12) Ye, C.; Zhang, Z.; Wang, Z.; Hua, Q.; Zhang, R.; Xie, X. Identification of a Novel Small-Molecule Agonist for Human G Protein-Coupled Receptor 3. *Journal of Pharmacology and Experimental Therapeutics* **2014**, *349* (3), 437–443.  
<https://doi.org/10.1124/jpet.114.213082>.
- (13) Laun, A. S.; Song, Z. H. GPR3 and GPR6, Novel Molecular Targets for Cannabidiol. *Biochem Biophys Res Commun* **2017**, *490* (1), 17–21.  
<https://doi.org/10.1016/j.bbrc.2017.05.165>.
- (14) Wu, J.; Chen, N.; Liu, Y.; Godlewski, G.; Kaplan, H. J.; Shrader, S. H.; Song, Z. H.; Shao, H. Studies of Involvement of G-Protein Coupled Receptor-3 in Cannabidiol Effects on Inflammatory Responses of Mouse Primary Astrocytes and Microglia. *PLoS One* **2021**, *16* (5 May).  
<https://doi.org/10.1371/journal.pone.0251677>.
- (15) Yin, H.; Chu, A.; Li, W.; Wang, B.; Shelton, F.; Otero, F.; Nguyen, D. G.; Caldwell, J. S.; Chen, Y. A. Lipid G Protein-Coupled Receptor Ligand Identification Using  $\beta$ -Arrestin PathHunter™ Assay. *Journal of Biological Chemistry* **2009**, *284* (18), 12328–12338.  
<https://doi.org/10.1074/JBC.M806516200>.
- (16) Uhlenbrock, K.; Gassenhuber, H.; Kostenis, E. Sphingosine 1-Phosphate Is a Ligand of the Human Gpr3, Gpr6 and Gpr12 Family of Constitutively Active G Protein-Coupled Receptors. *Cell Signal* **2002**, *14* (11), 941–953.  
[https://doi.org/https://doi.org/10.1016/S0898-6568\(02\)00041-4](https://doi.org/https://doi.org/10.1016/S0898-6568(02)00041-4).
- (17) Jensen, T.; Elster, L.; Nielsen, S. M.; Poda, S. B.; Loechel, F.; Volbracht, C.; Klewe, I. V.; David, L.; Watson, S. P. The Identification of GPR3 Inverse Agonist AF64394; The First Small Molecule Inhibitor of GPR3 Receptor Function. *Bioorg Med Chem Lett* **2014**, *24* (22), 5195–5198.  
<https://doi.org/10.1016/j.bmcl.2014.09.077>.
- (18) Ayukawa, K.; Suzuki, C.; Ogasawara, H.; Kinoshita, T.; Furuno, M.; Suzuki, G. Development of a High-Throughput Screening-Compatible Assay for Discovery of GPR3 Inverse Agonists Using a CAMP Biosensor. *SLAS Discovery* **2020**, *25* (3), 287–298.  
<https://doi.org/10.1177/2472555219875101>.
- (19) Gay, E. A.; Harris, D. L.; Wilson, J. W.; Blough, B. E. The Development of Diphenylethylidonium Analogs as GPR3 Agonists. *Bioorg Med Chem Lett* **2023**, *94*, 129427.  
<https://doi.org/10.1016/J.BMCL.2023.129427>.
- (20) Hall, M. P.; Unch, J.; Binkowski, B. F.; Valley, M. P.; Butler, B. L.; Wood, M. G.; Otto, P.; Zimmerman, K.; Vidugiris, G.; MacHleidt, T.; Robers, M. B.; Benink, H. A.; Eggers, C. T.; Slater, M. R.; Meisenheimer, P. L.; Klaubert, D. H.; Fan, F.; Encell, L. P.; Wood, K. V. Engineered Luciferase Reporter from a Deep Sea Shrimp Utilizing a Novel Imidazopyrazinone Substrate. *ACS Chem Biol* **2012**, *7* (11), 1848–1857.  
<https://doi.org/10.1021/cb3002478>.

- (21) Los, G. V.; Encell, L. P.; McDougall, M. G.; Hartzell, D. D.; Karassina, N.; Zimprich, C.; Wood, M. G.; Learish, R.; Ohana, R. F.; Urh, M.; Simpson, D.; Mendez, J.; Zimmerman, K.; Otto, P.; Vidugiris, G.; Zhu, J.; Darzins, A.; Klaubert, D. H.; Bulleit, R. F.; Wood, K. V. HaloTag: A Novel Protein Labeling Technology for Cell Imaging and Protein Analysis. *ACS Chem Biol* **2008**. <https://doi.org/10.1021/cb800025k>.
- (22) Schihada, H.; Vandenabeele, S.; Zabel, U.; Frank, M.; Lohse, M. J.; Maiellaro, I. A Universal Bioluminescence Resonance Energy Transfer Sensor Design Enables High-Sensitivity Screening of GPCR Activation Dynamics. *Commun Biol* **2018**, *1* (1). <https://doi.org/10.1038/s42003-018-0072-0>.
- (23) Schihada, H.; Nemeč, K.; Lohse, M. J.; Maiellaro, I. Bioluminescence in G Protein-Coupled Receptors Drug Screening Using Nanoluciferase and Halo-Tag Technology. In *Methods in Molecular Biology*; Humana Press Inc., 2021; Vol. 2268, pp 137–147. [https://doi.org/10.1007/978-1-0716-1221-7\\_9](https://doi.org/10.1007/978-1-0716-1221-7_9).
- (24) Schihada, H.; Ma, X.; Zabel, U.; Vischer, H. F.; Schulte, G.; Leurs, R.; Pockes, S.; Lohse, M. J. Development of a Conformational Histamine H3 Receptor Biosensor for the Synchronous Screening of Agonists and Inverse Agonists. *ACS Sens* **2020**, *5* (6), 1734–1742. <https://doi.org/10.1021/acssensors.0c00397>.
- (25) Zhang, J. H.; Chung, T. D. Y.; Oldenburg, K. R. A Simple Statistical Parameter for Use in Evaluation and Validation of High Throughput Screening Assays. *J Biomol Screen* **1999**, *4* (2), 67–73. <https://doi.org/10.1177/108705719900400206>.
- (26) Crousillac, S.; Colonna, J.; McMains, E.; Dewey, J. S.; Gleason, E. Sphingosine-1-Phosphate Elicits Receptor-Dependent Calcium Signaling in Retinal Amacrine Cells. *J Neurophysiol* **2009**, *102* (6), 3295–3309. <https://doi.org/10.1152/jn.00119.2009>.
- (27) Kolb, P.; Ferreira, R. S.; Irwin, J. J.; Shoichet, B. K. Docking and Chemoinformatic Screens for New Ligands and Targets. *Curr Opin Biotechnol* **2009**, *20* (4), 429–436. <https://doi.org/10.1016/j.copbio.2009.08.003>.
- (28) Hawkins, P. C. D.; Skillman, A. G.; Nicholls, A. Comparison of Shape-Matching and Docking as Virtual Screening Tools. *J Med Chem* **2007**, *50* (1), 74–82. <https://doi.org/10.1021/JM0603365>.
- (29) Backman, T. W. H.; Cao, Y.; Girke, T. ChemMine Tools: An Online Service for Analyzing and Clustering Small Molecules. *Nucleic Acids Res* **2011**, *39* (Web Server issue). <https://doi.org/10.1093/NAR/GKR320>.
- (30) Schihada, H.; Shekhani, R.; Schulte, G. Quantitative Assessment of Constitutive G Protein-Coupled Receptor Activity with BRET-Based G Protein Biosensors. *Sci Signal* **2021**, *14* (699), 1653. <https://doi.org/10.1126/scisignal.abf1653>.
- (31) Klarenbeek, J.; Goedhart, J.; Van Batenburg, A.; Groenewald, D.; Jalink, K. Fourth-Generation Epac-Based FRET Sensors for CAMP Feature Exceptional Brightness, Photostability and Dynamic Range: Characterization of Dedicated

Sensors for FLIM, for Ratiometry and with High Affinity. *PLoS One* **2015**. <https://doi.org/10.1371/journal.pone.0122513>.

- (32) Daina, A.; Michielin, O.; Zoete, V. SwissADME: A Free Web Tool to Evaluate

Pharmacokinetics, Drug-Likeness and Medicinal Chemistry Friendliness of Small Molecules. *Scientific Reports* **2017** *7:1* **2017**, *7* (1), 1–13. <https://doi.org/10.1038/srep42717>.

## Table of Contents artwork

